Nexus : Journal of Advances Studies of Engineering Science
ISSN: 2751-7578
Volume 03 Number 02 (2024)
https://innosci.org/index.php/JISES

Article

Harnessing the Power of Low-Altitude Platforms for Next-Gen Communication Technology of Unmanned Aerial Vehicles (UAVs)

Emad Jadeen Abdualsada Alshebaney[1]

1. Department of Electronics and Communications Engineering, Collage of Engineering, University of Al-Qadisiyah, Iraq
* Correspondence: emad.alshebaney@qu.edu.iq

Abstract: Low-altitude platform communication technology is a burgeoning field in telecommunications, offering diverse applications ranging from civilian to security and military domains. This technology is pivotal in providing communication services during network downtime, heavy traffic, natural disasters, or wartime scenarios. This paper explores the utilization of low-altitude platforms for telecommunications services, specifically focusing on mobile cellular networks, evaluating its performance through simulation software under various conditions.

Keywords: Power, Aerial Unmanned, Scenarios, Signal-to-interference, Amplitude

1. Introduction

The demand for telecommunications services is rising dramatically around the world, which has sped up the creation of new generations of communication systems that can reach anybody, anywhere, at any time. In order to accomplish this, it aims to offer coverage for these cellular service providers to be the greatest and the nearest. One of the most advanced and promising technologies in this industry is low-rise platform communication systems. The purpose of this study is to provide insight into low-height cross-platform communication systems.

This study is significant since it uses the previously indicated methodology. It is anticipated to have a substantial impact on quality improvement, which is one of the newest technologies, as well as the advancement of technological services in next-generation wireless communication systems, particularly in emergency situations or when the essential services cannot be supplied by the basic telecommunications networks.

Generally speaking, it has embraced the concept of using unmanned aerial aircraft (Aerial Unmanned UAV: aircraft) as network access points in conjunction with functional communication systems on low-rise platforms. These networks can be used for both military and civilian purposes; the military mostly uses them for border surveillance and reconnaissance. As it can be directed to the provision of telecommunications services for civilian use various public agencies and institutions such as police, traffic and public safety, the Department of Transport and Air Navigation, and Remote Sensing. It can also for communications over low-end platforms to provide an alternative when a network fails or public communications in the event of disasters or wars, which helps to accelerate rescue and repair operations [1-8].

Citation: Alshebaney, E. J. A. Harnessing the Power of Low-Altitude Platforms for Next-Gen Communication Technology of Unmanned Aerial Vehicles (UAVs). Nexus: Journal of Advances Studies of engineering Science 2024, 3(2), 6-21.

Received: 10th March 2024
Revised: 17th March 2024
Accepted: 24th March 2024
Published: 1st April 2024

2. Materials and Methods

2.1. Low-rise platform uses

Low-rise platform communication systems have many uses which include the provision of radio broadcasting and media communication services. Multiple services (voice, image, and data), as well as Internet and Internet services.

2.2. Low-rise platform systems' characteristics

Low-rise platform communication technology has many advantages.

The characteristics that make it one of the most promising technologies for communication systems for generations. Among these features, we mention the following points:

1) Low implementation costs: it is evident how much more expensive the equipment necessary to run these systems is compared to that needed for high-altitude platforms. The high price is justified by the fact that different performance criteria and requirements correlate with height, with demand increasing with height. To offer communication as though from a fixed base station, more sophisticated and costly equipment is required. Furthermore, in terms of installation and maintenance, the cost of communication systems on low-rise platforms is cheaper than that of the authorized system on base stations.
2) Communication time between users and low-altitude platforms to short the distance between. Short: This is due to the short time of propagation due to low-rise platforms and endpoints compared to a distance of deployment in existing high-altitude platform communication systems at an altitude of more than 20 km. From another point of view, we see that the higher the platform, the greater the signal will be attenuated because of the distance and the multiplicity of atmospheric layers that the signal penetrates, this is what low-rise platforms avoid; because of being in class lower part of the atmosphere.
3) Low altitude communication systems have a high potential for communication of Direct Line of Sight (LOS: Sight of Line), in comparison with terrestrial systems based on base stations; because of being taller in an environment than the various buildings and obstacles in the contact environment.
4) It is characterized by flexibility in the speed of its publication in the event of a request to provide its services in any place and time [9]

2.3. Obstacles Low-rise platform technologies face

Even with all the benefits and features that low-height platforms for communication technology offer, in order to remain a leader in the field, the upcoming generation will require additional research and development for these systems in order to provide answers to issues that arise with their widespread use. The following issues are a few of the difficulties that this technology's implementation and dissemination face:

1) Limited coverage area: Compared to the area covered by high-rise platforms, the coverage area of the platforms is insignificant due to their low height, which ranges only a few hundred meters.
2) Reflects variations in the weather, such as winds, rain, and other meteorological elements. For the same reasons that make it challenging to pinpoint the low-rise platform's precise location, it is crucial to launch and monitor the platform.
3) The age of the batteries limits how long the platform can stay in the air, although solar energy can generally solve this issue [10].

2.4. A mathematical depiction of aerial platform networks

This section of the paper gives a mathematical description of the key performance evaluation parameters of communications systems with low-altitude platforms, including how the coverage area is shaped, how signal strength to interference ratios are calculated, how many users can be served at once, and the system's overall capacity.

2.5. Cell formation

Low-altitude platforms can cover multiple cells on the Earth's surface, with each cell served by a distinct beam emitted from an array antenna. The shape of the coverage area can be delineated based on the beam width and platform footprint.

By elucidating the potential and challenges of low-altitude platform communication technology, this paper aims to contribute to the advancement of next-generation wireless communication systems, facilitating seamless connectivity in diverse scenarios airborne. Equation 1 outlines the description of this region's shape:

$$y = \pm h \tan(\emptyset_h) \cos(\theta_i)(1 + \frac{x}{h}\tan(\theta_i) \cdot \sqrt{1 - \left(\frac{1}{\tan(\theta_h)}\right)^2 \left\{\frac{\frac{x}{h} - \tan(\theta_i)}{1 + \frac{x}{h}\tan(\theta_i)}\right\}} \quad \ldots.(1)$$

In this context, "h" denotes the height of the airborne platform, while "∅" symbolizes the angle of rotation, and " θ " represents the angle of incidence of the ray. Furthermore, h" denotes the beam width on the ground, and the angle of view of the incident beam at the center of the power (BPH). Additionally, "x" represents the x-coordinate of the point within the coverage area extending from.

$$h \tan(\text{ø}_i - \text{ø}_h) \leq x \leq h \tan(\text{ø}_i - \text{ø}_h) \quad \ldots\ldots.(2)$$

Whereas, the y-coordinate of the point in the coverage area. And any point with known coordinates, it can be represented in the positive directions and the negative angle ∅ we get the new coordinates from the two equations:

$$x' = x \cos(\text{Ø}_k) - y \sin(\text{Ø}_k) \quad \ldots\ldots\ldots(3)$$

$$y' = y \cos(\text{Ø}_k) - x \sin(\text{Ø}_k) \quad \ldots\ldots\ldots(4)$$

If the diameter is denoted by "d" and is a function of both "θ" and "∅", where "h" represents the tangent of the angle "θh" and in this scenario, "hθ" denotes the angle of view for the central cell, the central radius of the cell can be calculated. For instance, when utilizing a platform of height equal to or greater than 500 and employing an array antenna consisting of 12 x 12 elements, with "N" denoting the beam width at mid-power (θh = BW∅ = 4.2482°), the central radius of the cell can be determined.

Thus the central radius of the cell can be calculated:

$$h \tan(\text{ø}_h) = 500 * \tan(4.2482) = 37.1m$$

Figure 1 illustrates the correlation between the angle of incidence of the beam and the beam width at mid-power. It is evident from the figure that as the angle of the radius increases (i.e., the distance from the terminal point of connection to the projected point increases), the width of the ray arriving at this point also increases. This could potentially lead to increased interference or a decreased signal-to-interference ratio (SIR) in areas distant from the platform.

To simplify the alignment of the curves, we can approximate the mathematical relationship between the angle of incidence and the width of the ray with the following equation cited in [10]:

$$\theta_h = 0.0735698\theta_i^{2.0000} + 0.08911 \quad (5)$$

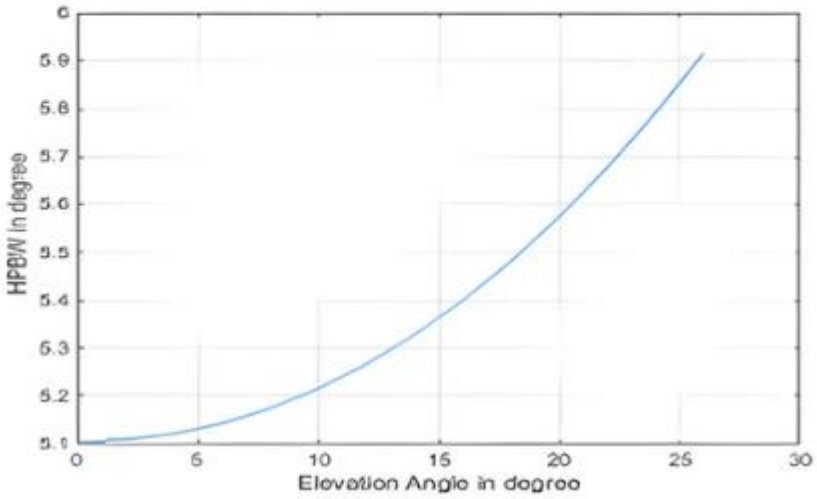

Figure 1. The correlation between the angle of incidence of the beam and the angle of the mid-power beam width (HPBW)

Furthermore, the cost of communication systems on low-rise platforms is lower than that of approved systems on base stations, considering installation and maintenance expenses.

2.6. Mathematical representation of Aerial Platform Networks

In this section of the study, the essential performance evaluation characteristics of communication systems utilizing low-altitude platforms, such as delineating the coverage area's shape, are depicted mathematically. This includes calculating the number of users that can be accommodated within the system's total capacity and determining the signal strength-to-interference ratio.

2.7. Formation of cells

Through the utilization of an array (multi-beam) antenna, the low-height platform can cover numerous terrestrial cells, each equipped with its own beam. Each beam possesses its unique angle of delineation, which encompasses a portion of the platform's geographical area towards a ground cell. Consequently, it can be inferred that the Airborne platform encompasses an area on the Earth's surface (footprint) for every beam of a known width. The description of this region's shape can be outlined as in [10]:

Where Gt represents the interference gain of the adjacent cell, G_r denotes the main ray gain for the primary cell (where the terminal user is located), and "j" signifies the number of adjacent cells to the primary interfering cell.

Determining the total number of users present, considering their shared utilization of system resources, can be computed using the following equation:

$$M = \frac{\left(\frac{E_b}{I_o}\right)\left(\frac{R_b}{B_c}\right)+1}{(1+\gamma)\left(\frac{E_b}{I_o}\right)\left(\frac{R_b}{B_c}\right)} \quad (7)$$

$$\gamma = \frac{1}{\text{SIR}} \quad (8)$$

Where E denotes the power per bit, I represents the interference power spectrum density, Io represents the power ratio of the interference to be obtained, R represents the data transmission rate (in bits per second), and Bc represents the transmission channel bandwidth.

2.8. Impact of path attenuation on signal integrity

The impact of path attenuation in open space on signals transmitted from airborne and aerial platforms can be determined using the following equation:

$$L_s = 20 \log (f_0) + 20 \log (d_L) - 147.56 \quad \ldots\ldots\ldots (9)$$

Here, f denotes the operating frequency (the frequency of the carrier signal), "m" represents the distance from the airborne platform to the user, and "dl" signifies the path loss in decibels (dB).

2.9. The calculation of the signal-to-noise and interference ratio

In order to enhance the accuracy and clarity of the results, this crucial factor has been incorporated into the system modeling calculations. The signal-to-noise and interference ratio can be determined using the following equation (10):

$$sin \frac{1}{\frac{1}{SIR}+\frac{1}{SNR}} \quad \ldots\ldots\ldots (10)$$

Where NS represents the ratio of the signal power to the noise power and is defined by the relationship:

$$SNR = \frac{pr}{pn} \quad \ldots\ldots\ldots (11)$$

Here, Pn refers to the noise power and Pr symbolizes the received power, which can be computed as follow

$$p_r = 10^{(p_t - L_s)/10} \quad \ldots\ldots\ldots (12)$$

Here, Pt is the transmitted power in decibels watts (dBW).

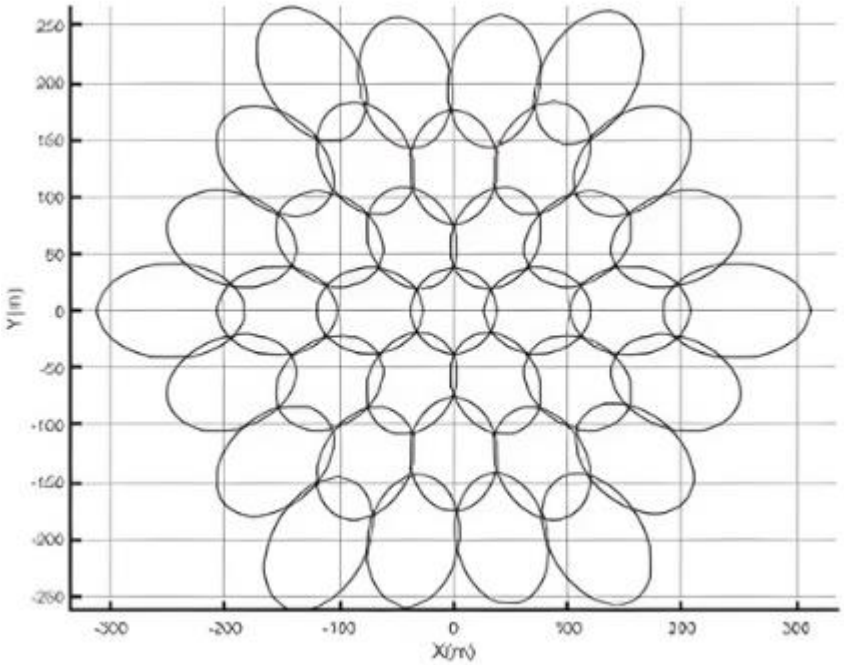

Figure 2. Illustration of the geographical coverage area of the low-altitude platform

To achieve the final depiction of the coverage area distribution for ground cells, as depicted in Figure 2, four angles of incidence for the rays were utilized, each corresponding to one of the 12 beams. By substituting these angles into equation (5), the width angle of the rays at mid-power directed towards each cell in the overall coverage area was determined.

3. Results

3.1. Explanation of sequential cells

As previously mentioned, each cell's coverage area is formed by a beam directed by the breadth of the airborne platform. Similar to Figure 3, point A represents the terminal node (M) of communication or mobile station, characterized by positional variability and denoted by ($\emptyset$, θ). The distance is measured from that point to the angular portable platform (Joe). The user serves as the focal point of interest, and the point "-" signifies the center of the adjacent area overlapping with the intended ray coverage area. Point A also denotes the center of the desired ray's coverage area.

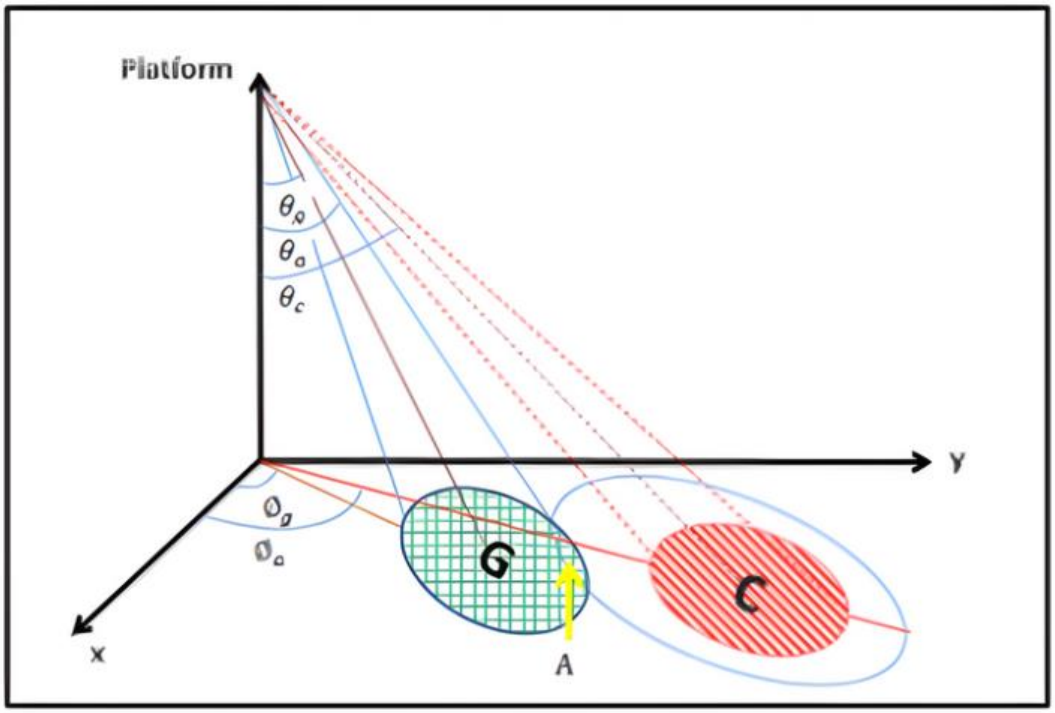

Figure 3. The region of user movement leading to overlap

3.2. Calculation of signal-to-interference ratio

The SIR in this system can be computed using the following equation:

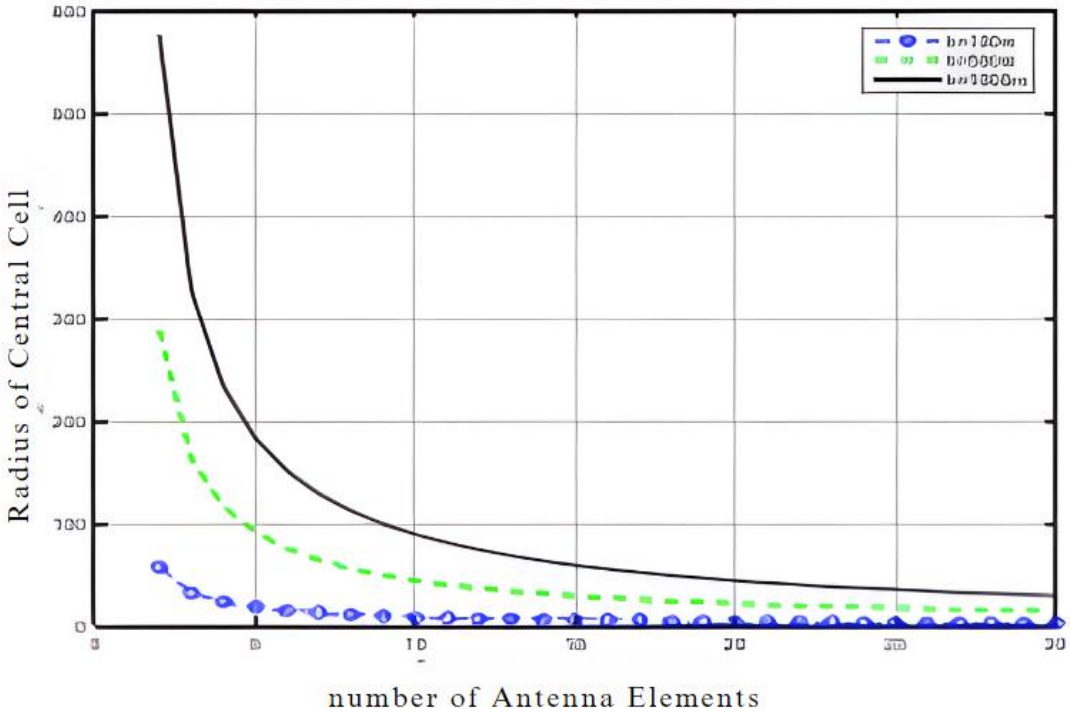

Figure 4. The central cell radius varies with alterations in the number of antenna elements (across different platform elevations)

3.3. Variation in user count with altered bandwidth and transmission rate

Examination of the attributes of communication systems employed by airborne platforms, specifically those of low-altitude platforms, as detailed in Table 1.

Table 1. Attributes of communication systems utilized by low-altitude airborne platforms

bandwidth	[4.1, 5, 20 [MHz
data transmission rate	[100,1000 [kilobits per second]
transmission capacity	20 Watt
Ambient temperature	30 c
Operating frequency	1800MHz
Signal-to-interference ratio $\boldsymbol{Eb/I}$(req.)	22.4 dB to − 6.7 dB m

The results of the simulation for this system are depicted in Figure 5, illustrating the correlation between the quantity of instantaneous users within the central cell and the signal-to-interference ratio (denoted as Eb/Io, essential for the system's equipment to operate at the requisite standard, ensuring communication quality at a specified level). The figure showcases this correlation across varying bandwidth values to achieve a transmission rate of 1 Mbps per user. Notably, the figure demonstrates that as the signal-to-interference ratio required for maintaining system functionality increases, the number of users diminishes. Similarly, a narrower bandwidth is associated with a reduced number of users. For instance, when comparing user allocation across different frequency bands, at a bandwidth of 20 MHz, 24 users can simultaneously communicate at a rate of 1 Mbps, whereas, with an increase in the desired signal-to-interference level (Eb/Io) to 3dB, each cell can only accommodate 12 users.

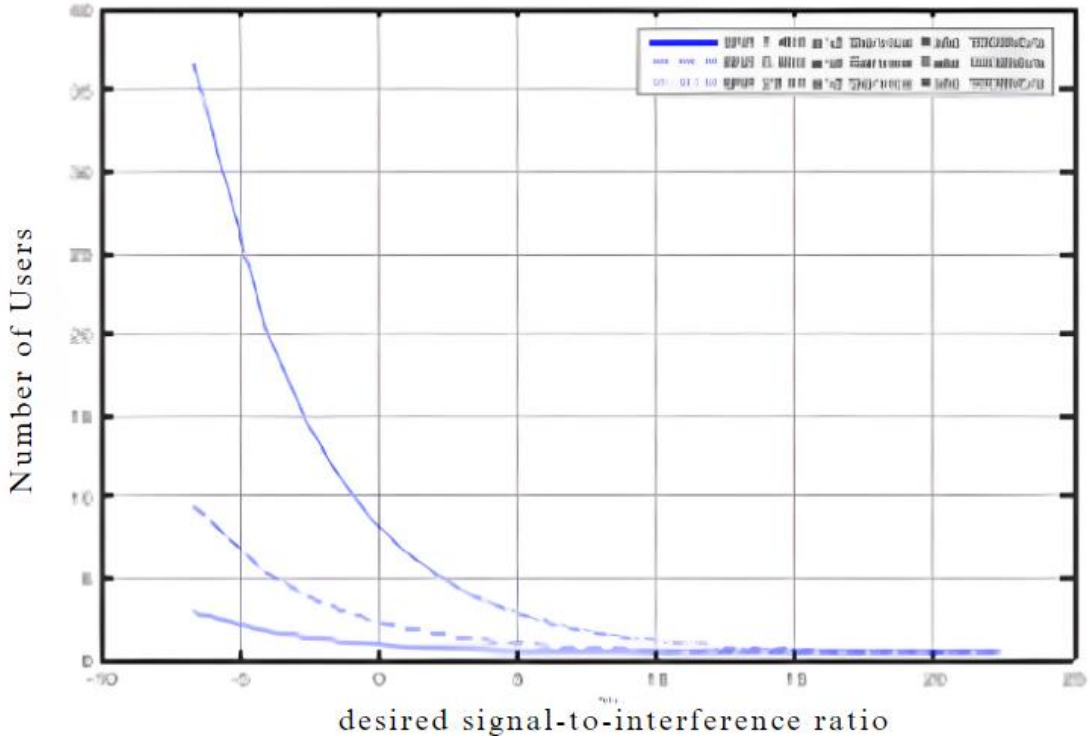

Figure 5. The relationship between the number of users and the desired signal-to-interference ratio across different bandwidths, maintaining a transmission rate of 1 Mbps

3.4. Capacity calculation

Shannon's mathematical formula is commonly used to calculate the capacity of a communication channel. However, in this context, we will express the system's spectral efficiency, representing the amplitude per hertz or the maximum transmission rate per hertz of the assigned bandwidth, using the equation:

$$c=\log_2=(1+SIN\ R) \quad \text{……. (13)}$$

3.5. Evaluation of Low-rise platforms' communication systems performance

This section evaluates the performance of communication systems in various low-altitude platform environments and compares these results with those of high-altitude platform installations and base station-based systems.

3.6. Connection between transmitted beam width and platform antenna count

The width angle of the beam at the power midpoint is critical for determining cell size in airborne platform communication systems. This beam width correlates with another vital aspect of platform design: the number of antennas used (N). Figure 6 illustrates this relationship by varying the number of antenna array members from 2 to 100. It's evident from the figure that the beam width decreases as the number of antennas increases.

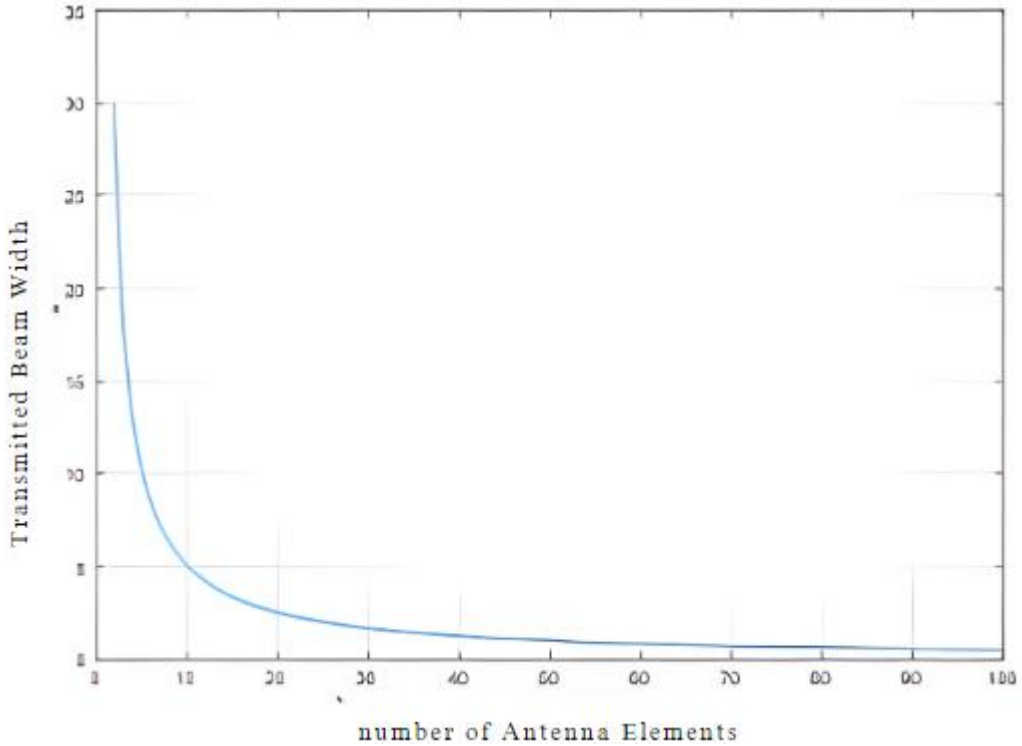

Figure 6. Variation of transmitted beam width with number of antenna elements on platform

As the size of cells is directly influenced by the beam width emitted from the platform, the number of antennas utilized indirectly impacts the cell radius within this system. The effect of adjusting the number of antenna elements on the cell radius was investigated. Figure 7 demonstrates the relationship between the radius of the central cell and the number of antennas employed in the platform across different heights, providing empirical evidence of this relationship. Consequently, it can be inferred that to accommodate more subscribers within the same area, the size of cells may need to be reduced when the platform reaches a certain height.

The maximum number of users per cell was two, each operating at a speed of two megabits per second. In contrast, the observed number of users was seventy-six, with each user transmitting at a speed of one hundred kilobits per second. Moreover, at a signal-to-interference ratio of -5 dB, the system could support a maximum of 246 users, each capable of transmitting at a speed of 100 kilobits per second, while the minimum number of users supported was 12 when the transmission rate was 2 megabits per second. This underscores

the importance of either enhancing the transmission rate or increasing the number of users within the system.

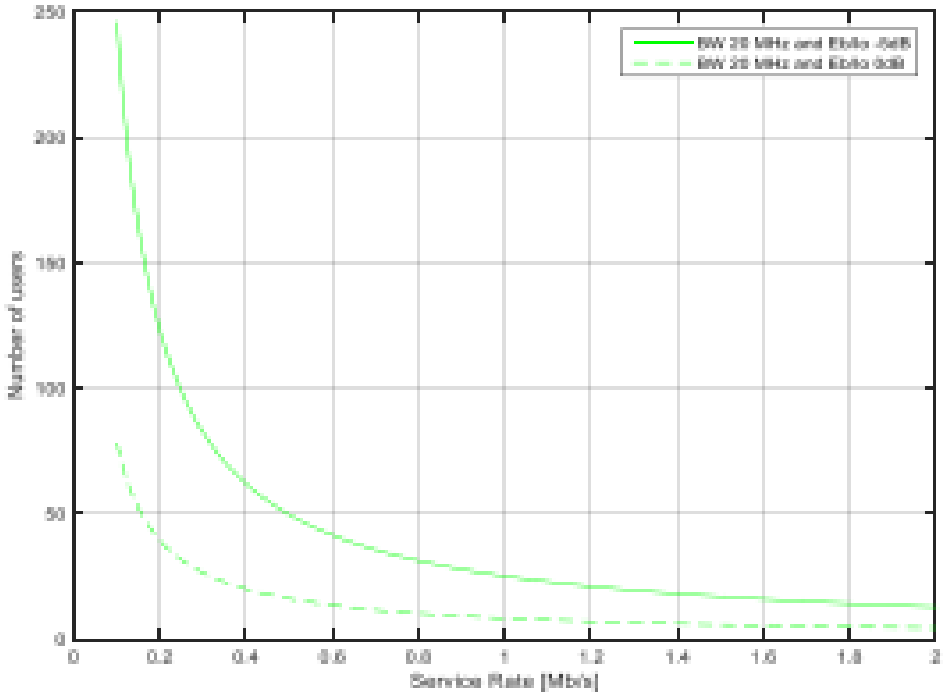

Figure 7. The number of users at a signal-to-interference ratio of *d*−0 *Eb/Io* with a 20MHz bandwidth

3.7. Examination of spectral efficiency and overall system capacity

Assessing the system's effectiveness, particularly when utilizing system bandwidth, becomes more straightforward when estimating the total capacity achievable by understanding the spatial distribution of spectral efficiency (amplitude per hertz) across the coverage area. While the cutoff probability of 50% represents the average amplitude within a cell generally, the communication channel's characteristics may vary. However, assuming an outage probability of 10% at the cell center and 90% at the cell's edge, simulation results reveal the total amplitude determined by the cutoff probability for each region, as outlined in Table 2.

Table 2. Outage probability distribution across cell regions based on simulation results

Medium capacity	**Capacitance at the edge of the cell**	**The capacitance at the center of the cell**	**Bandwidth**
2.041 Mbps	0920 Mbps	3.280 Mbps	1.4 MHz
7.29 Mbps	3.284 Mbps	11.715 Mbps	5 MHz
29.16 Mbps	13.136 Mbps	46.86 Mbps	20 MHz

3.8. Influence of variation in flying platform position on system performance

To introduce objectivity and realism into the system analysis, the effect of the airborne platform's horizontal deviation on the communication system's performance was quantified.

Subsequently, the comparison of user numbers was conducted under fixed values of Eb/Io at 0 and d at 5, utilizing varying bandwidths and transmission rates ranging from 100 Kbps to 2 Mbps. In the initial scenario illustrated in Figure 8, with a bandwidth of 4.1 MHz and a required signal-to-interference ratio d 0, Eb/Io, the maximum number of users was 5, each limited to communication speeds of 100 Kbps, with the minimum number of users being approximately one when the data transmission rate was set at 2 Mbps. Conversely, in the subsequent scenario where the required signal strength d 5 Eb/Io was -5, the maximum number of users increased to 17, each capable of communicating at a rate of 100 Kbps. However, with the transmission rate boosted to 2 Mbps, the number of users dwindled to a minimum, matching the first scenario with only one user.

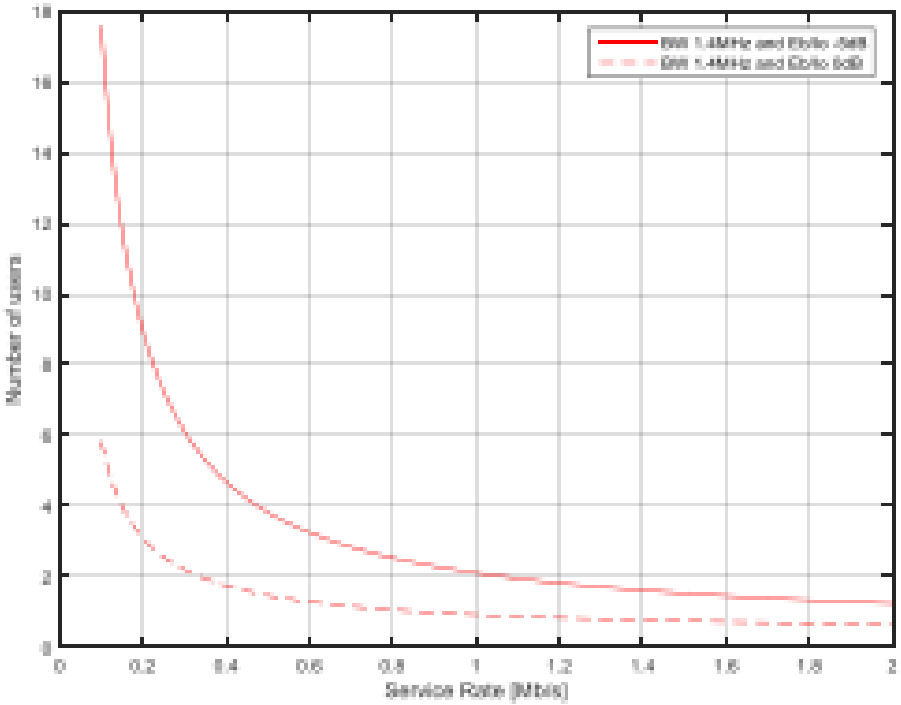

Figure 8. Number of users at a signal-to-interference ratio of d−0 Eb/Io and a bandwidth of 1.4 MHz

Conversely, the outcomes depicted in Figure 9 display the user count under a bandwidth allocation of 5MHz and d0 Eb/Io, where the maximum number of users reaches 19 at a data transmission rate of 100 kilobits per second, while the minimum number is a single user capable of achieving a rate of 2 megabits per second. For a signal-to-interference ratio of −5 Eb/Io, the maximum user count rises to 60 at a transmission rate of 100 kilobits per second, with a minimum of 3 users operating at a rate of 2 megabits per second.

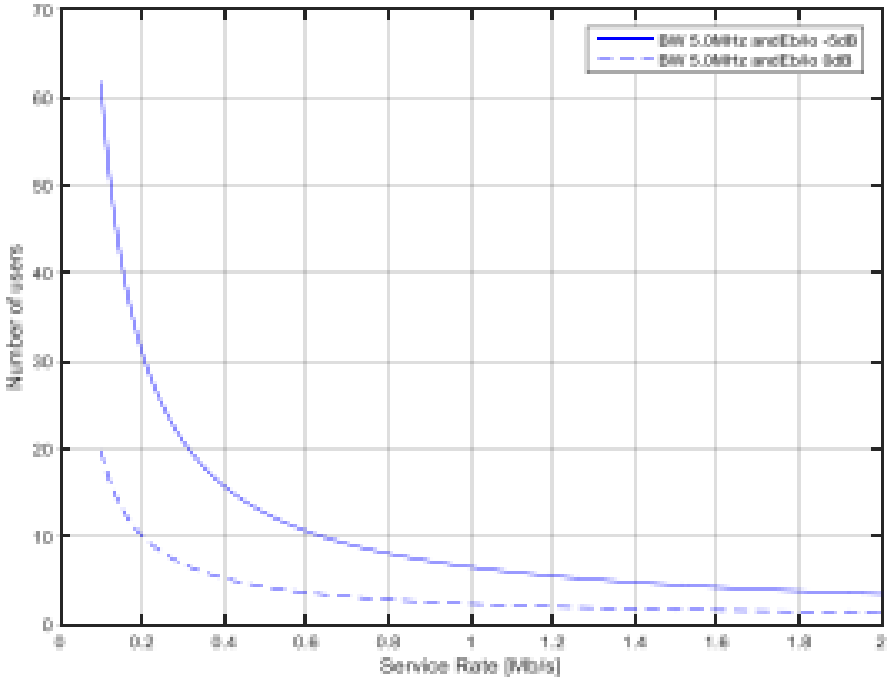

Figure 9. User count at Eb/Io = 0 with 5 MHz and 20 MHz Bandwidths: Illustrated results

At d 0 $Eb/=$, the maximum number of desired transmitting antennas remains constant, regardless of any alteration in the distance between the user and the interfering transmitting antenna, both of which are stationary on the same platform. However, it's essential to acknowledge the slight variations that may occur due to an enhanced signal-to-noise ratio when the platform height decreases.

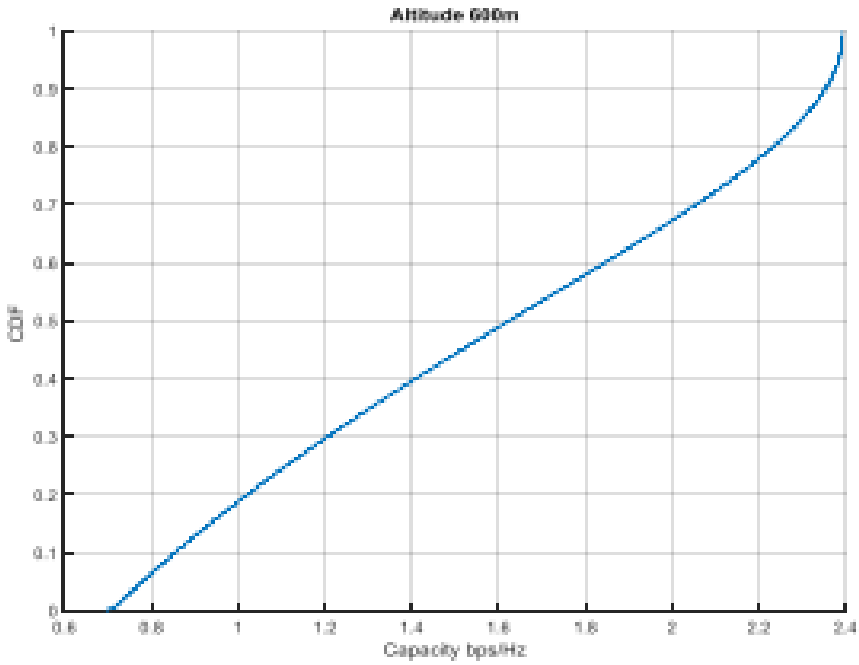

Figure 10. Spectral efficiency distribution at an Altitude of 600 meters

4. Discussion

4.1. Concluding remarks and findings

The low-rise platform systems explored in this study represent a modern wireless communication technology. Here, we outline the significant discoveries from our examination and evaluation of this technology's efficacy within cellular communication systems:

- Utilizing a platform equipped with an antenna array comprising 12 antennas revealed that alterations in height within a specified range lead to fluctuations in the ground coverage area. With a height of 500 meters, the covered area spanned approximately 250 meters in length and 300 meters in width.
- Variations in the number of array antennas on the platform directly impact the angle of the beam width at the mid-power (BPH''), resulting in changes in cell areas and the angle at which the beam reaches users. Consequently, user count and service quality exhibit disparities.
- Altering the bandwidth and signal-to-interference ratio operational levels affects the system differently. While wider bandwidths accommodate more users or offer increased transmission rates per user, system performance is further enhanced with upgraded equipment.
- It's evident that deviations from the exact platform position induce changes in ground angles and distances, as depicted in Figure 11. Consequently, recalculations are necessary to assess this effect. Anticipating performance shifts due to deviations, we assumed a platform displacement of 10 meters at a 30-degree angle. Table 3 summarizes the results post-adjustment, considering this deviation's impact.

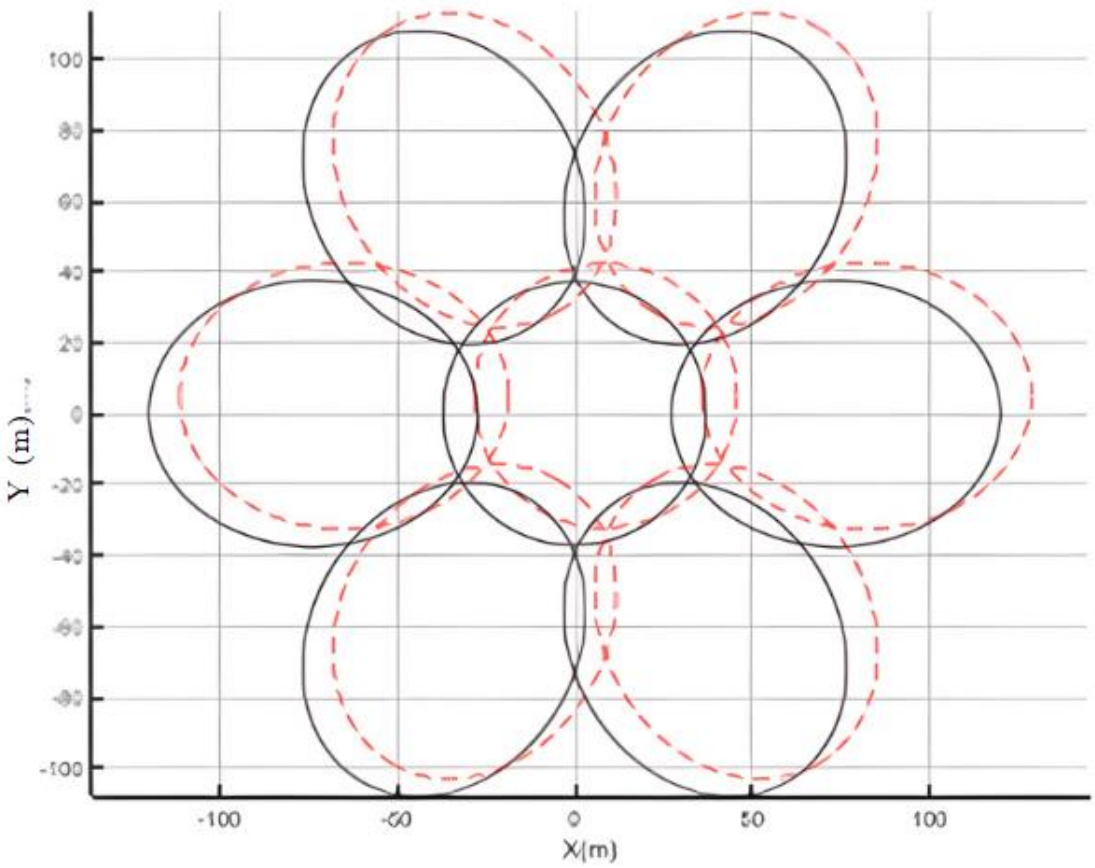

Figure 11. Impact of platform deviation on the geographic coverage area distribution

Table 3. Variation in capacity with platform deviation from exact position

Medium capacity	Capacitance at the edge of the cell	The capacitance at the center of the cell	Bandwidth
2.275 *Mbps*	1.201 *Mbps*	3.2984 *Mbps*	1.4 MHz
8.125 *Mbps*	4.289 *Mbps*	11.78 *Mbps*	5 MHz
32.5 *Mbps*	17.154 *Mbps*	47.12 *Mbps*	20 MHz

By contrasting the average total capacity in both scenarios—namely, under site discipline conditions and when the platform undergoes deviation—we observe a decrease in amplitude of approximately 10.3%, calculated as $\frac{32.5-29.1666}{32.5} * 100\% = 10.3\%$.

4.2. Influence of aerial platform height variation on communication system performance

In this section, we will illustrate how alterations in platform height impact the performance of the communication system. The rationale behind this is that adjusting the platform's height alters the distance between the user and the platform. Upon comparing the results obtained from varying the height of the airborne platform (12a, b), it becomes apparent that the spectral efficiency curve remains unchanged regardless of platform height adjustments, indicating a consistent user Signal-to-Interference Ratio (SIR) despite height fluctuations.

Furthermore, it was noted that the achieved capacity at the cell periphery differs from that in the center due to varying focal point distances, primarily influenced by the prevalence of peripheral users. This discrepancy signifies interference's impact on service quality within the system, resulting in capacity alterations.

The effect of horizontal deviation in the aerial platform's position manifests in the distribution of spectral efficiency, consequently influencing capacity. This alteration typically leads to a reduction in overall capacity, reflecting a negative impact.

A noteworthy discovery is that, with the interference's signal-to-measure ratio remaining constant despite height adjustments, it can be inferred that changes in altitude do not significantly affect amplitude. This assumption, however, disregards factors such as geographical coverage, dispersion, and noise levels.

Generally, increasing height correlates with amplified signal-to-interference ratio and noise levels. Conversely, lowering height enhances the intended signal strength relative to noise levels.

5. Suggestion

This article serves as an introductory exploration into the realm of low-altitude platform communication. We propose several avenues for further research in this domain, including:

- Conducting analytical research to comprehensively evaluate the communication system's performance, encompassing error rate calculations and service quality assessments. Simulation and implementation of an integrated communication system operating from low-rise platforms, compliant with initial fifth-generation specifications, are recommended to support this endeavor.
- Investigating the impact of random noise distribution on the system.
- Exploring the effects of tilting the platform at specific angles from the horizontal position.

6. Conclusion

This study operated under the assumption of a constant noise value.

- Given the assumption of direct line-of-sight communication in the study, it is recommended to assess the probability of establishing a direct line connection (LOS) versus other scenarios in different conditions.
- To gather data suitable for modeling the communication channel and generating more accurate results for evaluating system performance in real-world settings, it is also recommended to deploy this system in the field by constructing miniature communication setups and conducting comprehensive measurements.

REFERENCES

[1] S. Karapantazis and F. Pavlidou, "Broadband communications via high-altitude platforms: A survey," *IEEE Communications Surveys & …*, 2005, [Online]. Available: https://scholar.archive.org/work/mbaezapz7feovja7e3b6nydy2i/access/wayback/http://stuweb.ee.mtu.edu/~jrvijaye/High-Altitude-Platforms.pdf

[2] N. H. Motlagh, T. Taleb, and O. Arouk, "Low-altitude unmanned aerial vehicles-based internet of things services: Comprehensive survey and future perspectives," *IEEE Internet Things J*, 2016, [Online]. Available: https://ieeexplore.ieee.org/abstract/document/7572034/

[3] K. Mershad, H. Dahrouj, H. Sarieddeen, and ..., "Cloud-enabled high-altitude platform systems: Challenges and opportunities," *Frontiers in …*, 2021, doi: 10.3389/frcmn.2021.716265.

[4] S. C. Arum, D. Grace, and P. D. Mitchell, "A review of wireless communication using high-altitude platforms for extended coverage and capacity," *Comput Commun*, 2020, [Online]. Available: https://www.sciencedirect.com/science/article/pii/S0140366419313143

[5] H. Hariyanto, H. Santoso, and ..., "Emergency broadband access network using low altitude platform," *International Conference …*, 2009, [Online]. Available: https://ieeexplore.ieee.org/abstract/document/5417275/

[6] J. Tiemann, F. Schweikowski, and ..., "Design of an UWB indoor-positioning system for UAV navigation in GNSS-denied environments," *… conference on indoor …*, 2015, [Online]. Available: https://ieeexplore.ieee.org/abstract/document/7346960/

[7] L. Chen and L. Zhang, "Spectral efficiency analysis for massive MIMO system under QoS constraint: an effective capacity perspective," *Mobile Networks and Applications*, 2021, doi: 10.1007/s11036-019-01414-4.

[8] M. S. Alouini and A. J. Goldsmith, "Area spectral efficiency of cellular mobile radio systems," *IEEE Transactions on vehicular …*, 1999, [Online]. Available: https://ieeexplore.ieee.org/abstract/document/775355/

[9] L. Reynaud and T. Rasheed, "Deployable aerial communication networks: challenges for futuristic applications," *Proceedings of the 9th ACM symposium on …*, 2012, doi: 10.1145/2387027.2387030.

[10] B. El-Jabu and R. Steele, "Cellular communications using aerial platforms," *IEEE Transactions on vehicular …*, 2001, [Online]. Available: https://ieeexplore.ieee.org/abstract/document/933305/

[11] A. Al-Hourani, S. Kandeepan, and ..., "Optimal LAP altitude for maximum coverage," *IEEE Wireless …*, 2014, [Online]. Available: https://ieeexplore.ieee.org/abstract/document/6863654/

[12] X. You, "Towards 6G wireless communication networks: vision, enabling technologies, and new paradigm shifts," *Science China Information Sciences*, vol. 64, no. 1, 2021, doi: 10.1007/s11432-020-2955-6.

[13] S. Huang, "A commentary review on the use of normalized difference vegetation index (NDVI) in the era of popular remote sensing," *J For Res (Harbin)*, vol. 32, no. 1, 2021, doi: 10.1007/s11676-020-01155-1.

[14] P. Fozouni, "Amplification-free detection of SARS-CoV-2 with CRISPR-Cas13a and mobile phone microscopy," *Cell*, vol. 184, no. 2, pp. 323–333, 2021, doi: 10.1016/j.cell.2020.12.001.

[15] Z. Ma, "Multifunctional Wearable Silver Nanowire Decorated Leather Nanocomposites for Joule Heating, Electromagnetic Interference Shielding and Piezoresistive Sensing," *Angewandte Chemie - International Edition*, vol. 61, no. 15, 2022, doi: 10.1002/anie.202200705.

[16] D. C. Nguyen, "Federated Learning for Internet of Things: A Comprehensive Survey," *IEEE Communications Surveys and Tutorials*, vol. 23, no. 3, pp. 1622–1658, 2021, doi: 10.1109/COMST.2021.3075439.

[17] M. Wang, "Construction, mechanism and prospective of conductive polymer composites with multiple interfaces for electromagnetic interference shielding: A review," *Carbon N Y*, vol. 177, pp. 377–402, 2021, doi: 10.1016/j.carbon.2021.02.047.

[18] D. C. Nguyen, "6G Internet of Things: A Comprehensive Survey," *IEEE Internet Things J*, vol. 9, no. 1, pp. 359–383, 2022, doi: 10.1109/JIOT.2021.3103320.

[19] Y. Zhang, "Flexible Sandwich-Structured Electromagnetic Interference Shielding Nanocomposite Films with Excellent Thermal Conductivities," *Small*, vol. 17, no. 42, 2021, doi: 10.1002/smll.202101951.

[20] A. D. Boursianis, "Internet of Things (IoT) and Agricultural Unmanned Aerial Vehicles (UAVs) in smart farming: A comprehensive review," *Internet of Things (Netherlands)*, vol. 18, 2022, doi: 10.1016/j.iot.2020.100187.

[21] W. Xu, "FAST-LIO2: Fast Direct LiDAR-Inertial Odometry," *IEEE Transactions on Robotics*, vol. 38, no. 4, pp. 2053–2073, 2022, doi: 10.1109/TRO.2022.3141876.

[22] P. K. R. Maddikunta, "Unmanned Aerial Vehicles in Smart Agriculture: Applications, Requirements, and Challenges," *IEEE Sens J*, vol. 21, no. 16, pp. 17608–17619, 2021, doi: 10.1109/JSEN.2021.3049471.

[23] O. Friha, "Internet of Things for the Future of Smart Agriculture: A Comprehensive Survey of Emerging Technologies," *IEEE/CAA Journal of Automatica Sinica*, vol. 8, no. 4, pp. 718–752, 2021, doi: 10.1109/JAS.2021.1003925.

[24] Z. Lin, "Supporting IoT with Rate-Splitting Multiple Access in Satellite and Aerial-Integrated Networks," *IEEE Internet Things J*, vol. 8, no. 14, pp. 11123–11134, 2021, doi: 10.1109/JIOT.2021.3051603.

[25] U. Nepal, "Comparing YOLOv3, YOLOv4 and YOLOv5 for Autonomous Landing Spot Detection in Faulty UAVs," *Sensors*, vol. 22, no. 2, 2022, doi: 10.3390/s22020464.

[26] L. Benos, "Machine learning in agriculture: A comprehensive updated review," *Sensors*, vol. 21, no. 11, 2021, doi: 10.3390/s21113758.

[27] G. Messina, "Monitoring onion crop 'cipolla rossa di tropea calabria igp' growth and yield response to varying nitrogen fertilizer application rates using uav imagery," *Drones*, vol. 5, no. 3, 2021, doi: 10.3390/drones5030061.

[28] H. Peng, "Multi-Agent Reinforcement Learning Based Resource Management in MEC- And UAV-Assisted Vehicular Networks," *IEEE Journal on Selected Areas in Communications*, vol. 39, no. 1, pp. 131–141, 2021, doi: 10.1109/JSAC.2020.3036962.

[29] I. Kim, "Nanophotonics for light detection and ranging technology," *Nat Nanotechnol*, vol. 16, no. 5, pp. 508–524, 2021, doi: 10.1038/s41565-021-00895-3.

[30] Q. Wu, "A Comprehensive Overview on 5G-and-Beyond Networks with UAVs: From Communications to Sensing and Intelligence," *IEEE Journal on Selected Areas in Communications*, vol. 39, no. 10, pp. 2912–2945, 2021, doi: 10.1109/JSAC.2021.3088681.